Optical Materials xxx (xxxx) xxx–xxx

Contents lists available at ScienceDirect

Optical Materials

journal homepage: www.elsevier.com/locate/optmat

Coherent emission from fully Er^{3+} doped monolithic 1-D dielectric microcavity fabricated by rf-sputtering

A. Chiasera[a,*], C. Meroni[b,a], F. Scotognella[c,d], Y.G. Boucher[e], G. Galzerano[f], A. Lukowiak[g], D. Ristic[h], G. Speranza[i,a], S. Valligatla[j], S. Varas[a], L. Zur[k,a], M. Ivanda[h], G.C. Righini[k,l], S. Taccheo[m], R. Ramponi[f], M. Ferrari[a,k]

[a] IFN - CNR CSMFO Lab. & FBK CMM, Trento, Italy
[b] Dipartimento di Fisica, Università di Trento, Trento, Italy
[c] Politecnico di Milano, Dipartimento di Fisica and IFN-CNR, Milano, Italy
[d] Center for Nano Science and Technology@PoliMi, Istituto Italiano di Tecnologia, Milan, Italy
[e] Laboratoire FOTON (UMR CNRS 6082) Équipe Systèmes Photoniques, ENSSAT, F-22305, LANNION, France
[f] IFN – CNR and Politecnico di Milano, Dipartimento di Fisica, Milano, Italy
[g] Institute of Low Temperature and Structure Research, PAS, Wroclaw, Poland
[h] Center of Excellence for Advanced Materials and Sensing Devices, Ruđer Bošković Institute, Zagreb, Croatia
[i] FBK CMM FMPS Unit, Trento, Italy
[j] Institute for Integrative Nanosciences, IFW Dresden, Germany
[k] Enrico Fermi Center, Roma, Italy
[l] MiPLab. IFAC - CNR, Sesto Fiorentino, Italy
[m] College of Engineering, Swansea University, Swansea, UK

ARTICLE INFO

Keywords:
rf-sputtering
1-D dielectric microcavity
Silica
Titania
Erbium
Coherent emission

ABSTRACT

All Er^{3+} doped dielectric 1-D microcavity was fabricated by rf sputtering technique. The microcavity was constituted by half wave Er^{3+} doped SiO_2 active layer inserted between two Bragg reflectors consists of ten pairs of SiO_2/TiO_2 layers also doped with Er^{3+} ions. The scanning electron microscopy was used to check the morphology of the structure. Transmission measurements confirm the third and first order cavity resonance at 530 nm and 1560 nm, respectively. The photoluminescence measurements were obtained by optically exciting at the third order cavity resonance using 514.5 nm Ar^+ laser with an excitation angle of 30°. The Full Width at Half Maximum of the emission peak at 1560 nm decrease with the pump power until the spectral resolution of the detection system of ~1.0 nm. Moreover, the emission intensity presents a non-linear behavior with the pump power and a threshold at about 24 mW was observed with saturation of the signal at above 185 mW of pump power.

1. Introduction

Rare earth-activated glasses are one of the key materials in photonic systems because of their relevance for the development of optical amplifiers and light sources [1,2] and recently many effort was directed to develop appropriate material systems and configurations to exploit at the best luminescence properties of rare earth ions like Er^{3+} ions [3,4]. A possibility to enhance emission properties of emitters is given by tailoring their surrounding [5,6] and with this aim, several approaches, using nanocomposite materials or specific geometries, such as planar interfaces, photonic crystals, solid state planar microcavities, dielectric nanospheres, and spherical microresonators, have been proposed. Moreover, when only Er^{3+} ions are present in compact systems, the pumping scheme become crucial since the Er^{3+} absorption cross sections are not so high. To alleviate this issue various configuration is proposed such as addition of sensitizing ions of nanoparticles [7–10].

Among these different approaches and geometry, one-dimensional (1-D) photonic crystals, are the simplest photonic band-gap (PBG) device exploitable to manipulate the emission and absorption properties of rare earth ions [11–14] and they can be successfully used to obtain stimulated emission [15]. However, to obtain stimulated emission from an Erbium doped 1-D photonic crystals a careful tailoring of the geometry and involved materials are needed. The systems, in fact, require transparent materials at both excitation and emission wavelengths and the correct configuration to enhance the spectroscopic feature of the rare earth ions at all the involved wavelengths [14,16].

* Corresponding author.
E-mail address: alessandro.chiasera@ifn.cnr.it (A. Chiasera).

https://doi.org/10.1016/j.optmat.2018.04.057
Received 7 March 2018; Accepted 30 April 2018

Oxide-based dielectric materials are particularly suitable for fabricating active PBG structures because they have wide transparency from the ultraviolet to the near-infrared. Furthermore, oxide-based dielectric materials have good resistance to temperature, corrosion and radiation as well [17–19].

To fabricate dielectric-based 1-D photonic crystals with suitable geometry to influence the spectroscopic features of the embedded erbium ions at both excitation and emission wavelengths the control and reproducibility in the deposition of thin dielectric layers is mandatory. Processes like ion implanting [6], sol–gel [12,20], electron-beam evaporation [21], sputtering [13,14,17] can be successfully employed for the fabrication of microcavities based on oxide dielectric materials. However, to reach high quality factor Q using dielectric material, where the refractive indexes difference between the different materials is not so high as for the semiconductor, the real time control of the deposition process is mandatory to allow a precise tailor of the deposition rate and obtain a enough good uniformity in thickness [13,14]. We have demonstrated as the rf sputtering is a suitable technique for fabrication of dielectric microcavities and to deposit alternating layers of different materials activated by rare-earth ions with controlled refractive index and thickness [13,14].

However, in these configurations, the absorption of the pump beam and the optical gain-length product are limited owing to the short active regions of the vertical-cavity structures when only the defect layer is activated. It is demonstrated as an optically pumped organic vertical-cavity laser, in which the whole layer including the Bragg reflectors was doped with laser dye, the lasing threshold was reduced compared with a laser with undoped Bragg reflectors under similar conditions [22] and rf-sputtering is a suitable technique to fabricate films activated with by Er^{3+} ions [13,23]. Moreover, it is also known as PBG structures not only enhance the emission properties of the embedded active systems but such structures can successfully employed to enhance the absorption feature of systems [24].

In the present work, an Er^{3+} doped SiO_2/TiO_2 1D photonic crystal with all TiO_2 and SiO_2 layers doped Er^{3+} is fabricated with rf-sputtering technique and a suitable geometry and pumping scheme is proposed, taking advantage of the third order cavity resonance for the excitation and the fundamental for the detection, to put in evidence the possibility of coherent emission.

2. Experimental

1-D Er^{3+} doped dielectric microcavity is fabricated by RF sputtering technique. Thin films of SiO_2 and TiO_2 both doped with Er^{3+} are used to fabricate the microcavity. The samples were deposited on SiO_2 and Si substrates. The samples were deposited on Si was employed for scanning electron microscopy (SEM) and energy dispersive spectroscopy (EDS) measurements. The sample deposited on SiO_2 was employed for optical and spectroscopic measurements. The substrates were cleaned inside the rf sputtering deposition chamber by heating at 120 °C for 30′ just before the deposition procedure. The sputtering deposition of the films was performed by sputtering alternatively changing a $15 \times 5cm^2$ titania and $15 \times 5cm^2$ silica targets on which metallic erbium pieces were placed. The deposition time necessary to reach the appropriate thickness of the Bragg layers, are about 55 min for silica layer and 1 h 30 min for titania layers respectively. The deposition time necessary to reach the appropriate thickness of the silica defect layer, to obtain the cavity resonance centered at 1560 nm is about 1 h 55 min. The residual pressure before the deposition is 4.5×10^{-7} mbar. During the deposition procedure, the substrates were not heated and the temperature of the sample holder during the deposition is 30 °C. The sputtering occurred with an Ar gas pressure of 5.4×10^{-3} mbar, the applied rf power was 150 W and 130 W for silica and titania targets respectively. To monitor the thickness of the layers during the deposition, two quartz microbalances Inficon instruments thickness monitor model SQM-160, faced on the two targets were employed. Thickness monitor was calibrated for the two kinds of materials by a long deposition process (24 h of deposition) and by directly measuring the thickness of the deposited layer by an m-line apparatus [25]. The final resolution on the effective thickness obtained by this quartz microbalance is about 1 Å. More details are available in reference [14]. The samples were heat treated at 400 °C for 6 h using the conventional oven.

The compositional analysis was performed using EDS, employing a Oxford mod. INCA PentaFETx3 apparatus. EDS measurement was employed in particular to quantify the Erbium content in each layer. SEM was used to analyze the morphology of the multi layer films and thickness of each layer. The cross section of the microcavity was analyzed by a FEG mod. JEOL JSM-7001 F apparatus at 15 kV after covering the films with a 20 nm gold layer.

The transmittance measurement of the cavity in the NIR and visible region at zero degree of incident angle was obtained by using a double beam Varian-Cary spectrophotometer.

The spectroscopic features of the Er^{3+} doped dielectric microcavity were investigated upon excitation at 514.5 nm using the line of an Ar^{+} ion laser and upon excitation at 980 nm using a diode laser. A convex lens of 20 cm focal length was used to focus the excitation beam on the microcavity with a spot of about 100 μm for the 514.5 nm excitation wavelength and of about 250 μm for the 980 nm excitation. The angle of excitation was carefully chosen at 30° to match the third order cavity resonance in case of 514.5 nm excitation. The photoluminescence from the microcavity was detected at 0° from the normal on the samples, with a solid angle of 10^{-1} sr. The emission was dispersed by a 320 mm single-grating monochromator with a resolution of 1 nm. The light was detected by using a Hamamatsu photomultiplier tube and standard lock-in technique. The excitation power of the incident beam was controlled by using neutral density filters. More details about the experimental set up can be found here [14].

3. Results

SEM micrograph of the all Er^{3+} doped 1D dielectric microcavity cross section is reported in Fig. 1. The structure consists of 10 pairs of SiO_2/TiO_2 layers on each Bragg mirror with a central defect layer of SiO_2 doped with Er^{3+}. The dark regions showed in Fig. 1 correspond to the SiO_2 layer and the bright regions correspond to the TiO_2 layer. The substrate is located at the bottom of the image and the air on the top. It is possible to identify the defect layer and the two Bragg reflectors. EDS measurements indicate that the Erbium content in all the layers is about 0.3 ± 0.1 mol%. The thickness and refractive indices of SiO_2, TiO_2 thin films were measured using m-line technique in the 1.5 μm range [13,25] on reference single SiO_2 and TiO_2 films fabricated using the protocol employed for the photonic crystal. The refractive indices for SiO_2 and TiO_2 are 1.44 and 2.2 respectively. The thickness of each layer

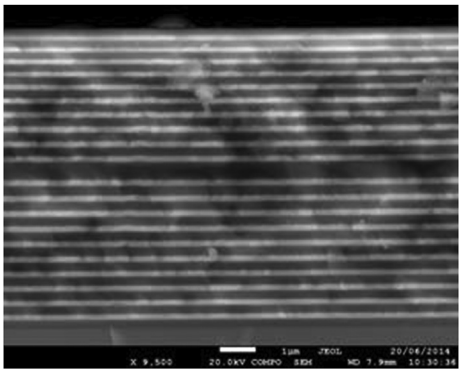

Fig. 1. SEM micrograph of the Er^{3+} doped 1D dielectric microcavity cross section. The bright and dark region corresponds to TiO_2 and SiO_2 layers, respectively. The substrate is located on the bottom of the images and air on the top.

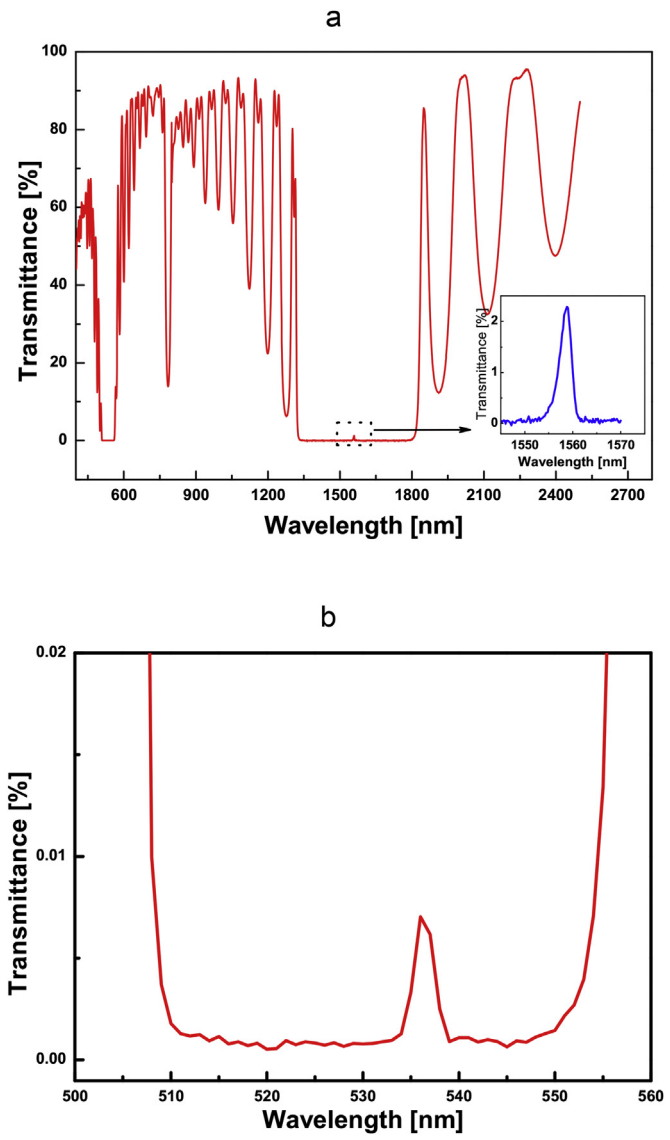

Fig. 2. (a) Transmission spectrum of the cavity with two Bragg mirrors, each one consisting of ten pairs of SiO_2/TiO_2 layers in the region between 450 nm and 2500 nm. The first order stop band ranges from 1300 nm to 1850 nm. The first order cavity resonance corresponds to the sharp maximum centered at 1559.2 nm. The incident light is unpolarized. (b) Transmission spectra representing third order stop band in the visible region between 500 nm and 560 nm with third order cavity resonance at 536 nm.

was monitored during the deposition using the quartz microbalance. The final thickness of each layer measured by SEM microscopy on the Bragg mirror was 270 ± 5 and 170 ± 5 nm for the silica and titania layers, respectively, and a thickness of 540 ± 5 nm for the SiO_2 doped with Er^{3+} defect layer.

The transmittance spectra of the sample are reported in Fig. 2. It is possible to identify the stop band from 1320 nm to 1830 nm is shown in Fig. 2(a). A sharp peak in the transmission spectra appears at 1559 nm corresponds to the cavity resonance related to the Er^{3+} doped SiO_2 half wave layer inserted between two Bragg mirrors. The inset graph shows the transmission spectrum obtained with resolution of 1 nm, shows the resonance line. It is also possible to observe the third order stop band in the visible region reported, enlarged, in Fig. 2(b), the third order of the cavity resonance is also presents in the stop band and appears at 530 nm at 0° incident angle. The third order stop band presents in the visible region and the cavity resonance appears at 530 nm at 0° incident angle. At 30° incident angle, the cavity resonance shifted to 514.5 nm.

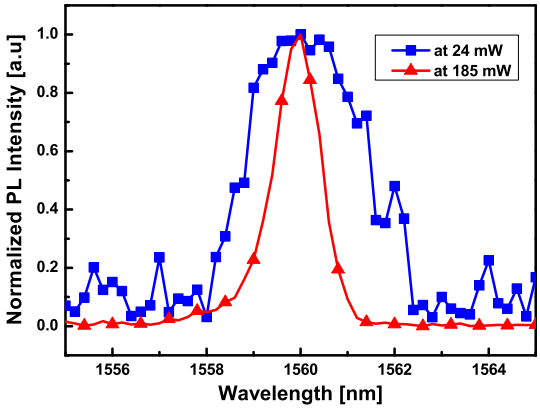

Fig. 3. $^4I_{13/2} \rightarrow {}^4I_{15/2}$ photoluminescence spectrum of the cavity activated by Er^{3+} ions in 1D dielectric microcavity. The emission is recorded at 0° from the normal on the samples upon excitation at 514.5 nm at the input power of 185 mW (red line) and 24 mW (blue line). (For interpretation of the references to colour in this figure legend, the reader is referred to the Web version of this article.)

Fig. 3 is reported the photoluminescence spectra related to the $^4I_{13/2} \rightarrow {}^4I_{15/2}$ transition of the Er^{3+} ions obtained for the microcavity at excitation power at 514.5 nm of 185 mW and 24 mW focalized on the sample. The erbium emission from the microcavity is centered at 1560 nm with Full Width at Half Maximum FWHM of ~1.0 ± 0.1 nm that correspond to the resolution of the detection apparatus in the case of excitation power of 185 mW while with 24 mW the FWHM correspond to 2.5 ± 0.1 nm.

In order to determine the behavior of the features of the emission with the excitation power, we evaluated the dependence of the emission intensity and FWHM with the 514.5 nm pump power. In Fig. 4 are reported the behavior of the emission intensity at emission wavelength of 1560 nm and FWHM as a function of different 514.5 nm excitation powers with a detection angle of 0° and an excitation angle of 30°.

In Fig. 5 is reported the behavior of the emission intensity at emission wavelength of 1560 nm with a detection angle of 0° and FWHM as a function of different 980 nm excitation powers.

4. Discussion

From the behavior of the emission intensity at emission wavelength of 1560 nm and FWHM as a function of different 514.5 nm excitation powers with a detection angle of 0° and an excitation angle of 30° it is

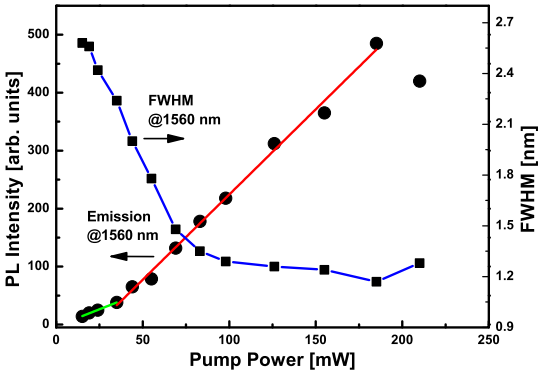

Fig. 4. $^4I_{13/2} \rightarrow {}^4I_{15/2}$ photoluminescence peak intensity and FWHM (blue line) at 1560 nm as a function of 514.5 nm pump power with 0° of detection angle and 30° of excitation angle. Red and green line are the results of linear fit while the blue line is a guide for the eyes. (For interpretation of the references to colour in this figure legend, the reader is referred to the Web version of this article.)

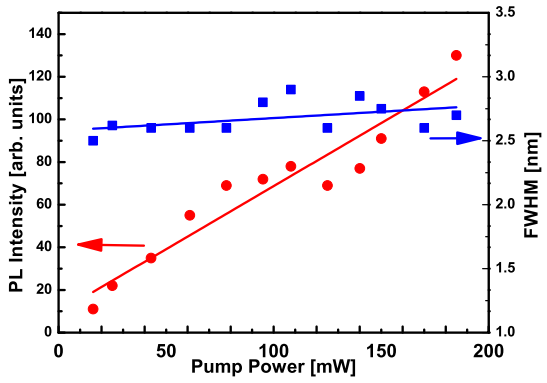

Fig. 5. $^4I_{13/2} \rightarrow {}^4I_{15/2}$ photoluminescence peak intensity (red) and FWHM (blue) at 1560 nm as a function of 980 nm pump power with 0° of detection angle and 30° of excitation angle. The blue and red lines are the results of linear fit. (For interpretation of the references to colour in this figure legend, the reader is referred to the Web version of this article.)

possible to observe that the intensity behavior is not linear but 3 different behavior can be highlighted: (I) below 30 mW of excitation power the peak intensity is linear and at 0 pump power reach 0 intensity; (II) between 30 and 180 mW the peak intensity is again linear but with different pendency than before and the red line that represent the linear fit in this region intercept the x-axis at a value of pump power of 24 mW; (III) above a pump power of 185 mw it is reach a saturation point and the intensity of the emission peak lean to decrease, it is important to note that reducing again the pump power below this saturation point the intensity climb up again. Simultaneously there is a narrowing of the FWHM from 2.5 nm at low pump power to around 1 nm which is limited by a spectral resolution of our experimental set up. In the same experimental conditions, we also carried out the photoluminescence measurements by exciting at 980 nm in order to check the emission characteristics also for this pumping scheme.

It is worthy of attention that using the 980 nm excitation it is not possible to find excitation angles that allow to match a resonance cavity order with the laser line. In this configuration, as reported in Fig. 5, the emission intensity vs input power graph is linear and the FWHM is constant at about 2.6 ± 0.1 nm. The same behavior, with linear dependency of the peak intensity with the excitation power and constant FWHM is obtained pumping at 514.5 nm but with an angle different from 30° therefore without exciting directly the third order of the cavity resonance.

Luminescence decay curves from the $^4I_{13/2}$ state of Er^{3+} ion obtained recording the signal by a digital oscilloscope, with excitation power at 514.5 nm of 185 mW focalized on the sample, show a lifetime of 300 μs that is close to the time resolution of the acquisition system. In the case of excitation at 514.5 nm with a power of 24 mW the signal is too low to allow the recording of the decay curve behavior but exciting at 980 nm with power of 200 mW it is possible record the decay curve. Also in this configuration the measured lifetime is of around 300 μs as obtained upon excitation at 514.5 nm with power of 185 mW, that is one order of magnitude lower than the expected values of the lifetime of the $^4I_{13/2}$ level of Er^{3+} ions in SiO_2 [26] and TiO_2 [27] matrices. We need to consider that is already observed in active microcavity [28] also doped with rare earth ions [29] a drastic decrease of the spontaneous emission lifetime with a decreasing that depends on the quality factor of the structures. These results indicate as a more time resolved characterization is needed for the complete characterization of such structures.

5. Conclusions

A protocol based on rf-sputtering technique for the fabrication of a monolithic, fully doped Er^{3+} dielectric 1-D microcavity was defined. The geometry of the structure is tailored to obtain the first order cavity resonance at 1560 nm at 0° of detection and the third order of the resonance at 514.5 nm at 30° respectively in order to match respectively the emission in the NIR region of the Er^{3+} ions and the green Ar^+ laser line in the visible region for the excitation of the Er^{3+} ions. Luminescence measurements demonstrate as the FWHM of the emission peak intensity at 1560 nm decrease with the pump power until the spectral resolution of the detection system of ~1.0 nm. Moreover the emission intensity present a non-linear behavior with the pump power and a threshold at about 24 mW was observed with saturation of the signal at 180 mW of pump power when excited in the third harmonic cavity resonance. Upon excitation with 980 nm or upon 514.5 nm but with an angle that do not allow the super impose the third harmonic cavity resonance, the luminescence measurements indicate a linear behavior of the emission peak at 1560 nm and a constant FWHM with the excitation power. The results suggest the presence of coherent emission from the sample and further measurements are in progress to define the temporal dynamics of this emission.

Acknowledgement

This research is performed in the framework of the projects: COST MP1401 “Advanced Fibre Laser and Coherent Source as tools for Society, Manufacturing and Lifescience” (2014–2018), ERANET-LAC FP7 Project RECOLA - Recovery of Lanthanides and other Metals from WEEE (2017–2019), MiFo Centro Fermi (2017–2020).

References

[1] M. Ferrari, G.C. Righini, N.S. Hussain, J. Da Silva Santos (Eds.), Physics and Chemistry of Rare-earth Ions Doped Glasses, Trans Tech Publishers, Pfaffikon, 2008, pp. 71–107.
[2] J.D.B. Bradley, M. Pollnau, Erbium-doped integrated waveguide amplifiers and lasers, Laser Photon. Rev. 5 (2011) 368–403.
[3] C.M. Johnson, P.J. Reece, G.J. Conibeer, Slow-light-enhanced upconversion for photovoltaic applications in one-dimensional photonic crystals, Opt. Lett. 36 (2011) 3990–3992.
[4] M.C. Gonçalves, L.M. Fortes, R.M. Almeida, A. Chiasera, A. Chiappini, M. Ferrari, Photoluminescence in Er^{3+}/Yb^{3+}-doped silica-titania inverse opal structures, J. Sol. Gel Sci. Technol. 55 (2010) 52–58.
[5] E. Snoeks, A. Lagendijk, A. Polman, Measuring and modifying the spontaneous emission rate of erbium near an interface, Phys. Rev. Lett. 74 (1995) 2459–2462.
[6] A.M. Vredenberg, N.E.J. Hunt, E.F. Schubert, P.C. Becker, D.C. Jacobson, J.M. Poate, G.J. Zydzik, Erbium implantation in optical microcavities for controlled spontaneous emission, Nucl. Instrum. Meth. B 74 (1993) 84–88.
[7] X. Orignac, D. Barbier, X. Min Du, R.M. Almeida, O. Mc Carthy, E. Yeatman, Sol–gel silica/titania-on-silicon Er/Yb-doped waveguides for optical amplification at 1.5 μm, Opt. Mater. 12 (1999) 1–18.
[8] M.P. Hehlen, N.J. Cockroft, T.R. Gosnell, A.J. Bruce, Spectroscopic properties of Er^{3+} -and Yb^{3+} -doped soda-lime silicate and aluminosilicate glasses, Phys. Rev. B 56 (1997) 9302–9318.
[9] C. Strohhöfer, A. Polman, Silver as a sensitizer for erbium, Appl. Phys. Lett. 81 (2002) 1414–1416.
[10] H. Portales, M. Mattarelli, M. Montagna, A. Chiasera, M. Ferrari, A. Martucci, P. Mazzoldi, S. Pelli, G.C. Righini, Investigation of the role of silver on spectroscopic features of Er3+-activated Ag-exchanged silicate and phosphate glasses, J. Non-Cryst. Solids 351 (2005) 1738–1742.
[11] H. Rigneault, C. Amra, S. Robert, C. Begon, F. Lamarque, B. Jacquier, P. Moretti, A.M. Jurdyc, A. Belarouci, Spontaneous emission into planar multi-dielectric microcavities: theoretical and experimental analysis of rare earth ion radiations, Opt. Mater. 11 (1999) 167–180.
[12] J. Jasieniak, C. Sada, A. Chiasera, M. Ferrari, A. Martucci, P. Mulvaney, Sol–gel based vertical optical microcavities with quantum dot defect layers, Adv. Funct. Mater. 18 (2008) 3772–3779.
[13] A. Chiasera, R. Belli, S.N.B. Bhaktha, A. Chiappini, M. Ferrari, Y. Jestin, E. Moser, G.C. Righini, C. Tosello, High quality factor Er^{3+}-activated dielectric microcavity fabricated by rf sputtering, Appl. Phys. Lett. 89 (2006) 171910–171911/3.
[14] S. Valligatla, A. Chiasera, S. Varas, N. Bazzanella, D.N. Rao, G.C. Righini, M. Ferrari, High quality factor 1-D Er^{3+}-activated dielectric microcavity fabricated by RF-sputtering, Optic Express 20 (2012) 21214–21224.
[15] A. Settimi, S. Severini, C. Sibilia, M. Bertolotti, A. Napoli, A. Messina, Coherent control of stimulated emission inside one dimensional photonic crystals: strong coupling regime, Eur. Phys. J. B 50 (2006) 379–391.
[16] Y. Gong, M. Makarova, S. Yerci, R. Li, M. Stevens, B. Baek, S. Nam, R. Hadfield, S. Dorenbos, V. Zwiller, J. Vučković, L. Negro, Linewidth narrowing and Purcell enhancement in photonic crystal cavitieson an Er-doped silicon nitride platform, Optic Express 18 (2010) 2601–2612.

[17] S.F. Chichibu, T. Ohmori, N. Shibata, T. Koyama, Dielectric SiO_2/ZrO_2 distributed Bragg reflectors for ZnO microcavities prepared by the reactive helicon-wave-excited-plasma sputtering method, Appl. Phys. Lett. 88 (2006) 161914–1-161914-3.
[18] L. Persano, P. Del Carro, E. Mele, R. Cingolani, D. Pisignano, Monolithic polymer microcavity lasers with on-top evaporated dielectric mirrors, Appl. Phys. Lett. 88 (2006) 121110–121111-121110-3.
[19] Y. Li, R.M. Almeida, Photoluminescence from a Tb-doped photonic crystal microcavity for white light generation, J. Phys. D Appl. Phys. 43 (2010) 455101–1-455101-7.
[20] Y. Li, L.M. Fortes, A. Chiappini, M. Ferrari, R.M. Almeida, High quality factor Er-doped Fabry–Perot microcavities by sol–gel processing, J. Phys. D Appl. Phys. 42 (2009) 205104–1-205104-7.
[21] G. Ma, J. Shen, Z. Zhang, Z. Hua, S.H. Tang, Ultrafast all-optical switching in one-dimensional photonic crystal with two defects, Optic Express 14 (2006) 858–865.
[22] H. Sakata, H. Takeuchi, K. Natsume, S. Suzuki, Vertical-cavity organic lasers with distributed-feedback structures based on active Bragg reflectors, Optic Express 14 (2006) 11681–11686.
[23] A. Chiasera, C. Armellini, S.N.B. Bhaktha, A. Chiappini, Y. Jestin, M. Ferrari, E. Moser, A. Coppa, V. Foglietti, P.T. Huy, K. Tran Ngoc, G. Nunzi Conti, S. Pelli, G.C. Righini, G. Speranza, Er^{3+}/Yb^{3+}-activated silica-hafnia planar waveguides for photonics fabricated by rf-sputtering, J. Non-Cryst. Solids 355 (2009) 1176–1179.
[24] K. Sakoda, Optical Properties of Photonic Crystals, Springer, Berlin, 2005.
[25] S.J.L. Ribeiro, Y. Messaddeq, R.R. Gonçalves, M. Ferrari, M. Montagna, M.A. Aegerter, Low optical loss planar waveguides prepared in an organic–inorganic hybrid system, Appl. Phys. Lett. 77 (2000) 3502–3504.
[26] W.J. Miniscalco, Erbium-doped glasses for fiber amplifiers at 1500 nm, J. Light wave Tech 9 (1991) 234–250.
[27] A. Bahtat, M.C. Marco de Lucas, B. Jacquier, B. Varrel, M.B. ouazaoui, J. Mugnier, IR luminescence decays and radiative lifetime of the $^4I_{sol132}$ level in Er^{3+} doped sol-gel TiO_2 planar waveguides, Opt. Mater. 7 (1997) 173–179.
[28] Y. Hanamaki, H. Akiyama, Y. Shiraki, Spontaneous emission alteration in InGaAs/GaAs vertical cavity surface emitting laser (VCSEL) structures, Semicond. Sci. Technol. 14 (1999) 797–803.
[29] A. Belarouci, F. Menchini, B. Jacquier, P. Moretti, H. Rigneault, S. Robert, Luminescence properties of Pr3+-doped optical microcavities, J. Lumin. 83–84 (1999) 275–282.